Physicochem. Probl. Miner. Process., 62(6), 2026, 242673

http://www.journalssystem.com/ppmp

Physicochemical Problems of Mineral Processing

ISSN 1643-1049
© Wroclaw University of Science and Technology

Selective flotation separation of molybdenite and galena using a maleic acid–acrylic acid copolymer as an eco-friendly depressant

Jiawei Huang [1,2,3], Xuekun Tang [1,2,3], Xianping Luo [1,2,3,4], Yang Siqi [1,2,3], Zishuai Liu [1,2,3], Chen Cheng [1,2,3]

[1] School of Mining Engineering, Jiangxi University of Science and Technology, Ganzhou 341000, China

[2] Jiangxi Provincial Key Laboratory of Low-Carbon Processing and Utilization of Strategic Metal Mineral Resources, Ganzhou 341000, China

[3] Jiangxi Province Green and Low-Carbon Development Industrial Technology Engineering Center for Lithium Resources, Ganzhou 341000, China

[4] National Key Laboratory of Uranium Resources Exploration-Mining and Nuclear Remote Sensing, East China University of Technology, Nanchang, Jiangxi 330013, China

Corresponding authors: txk0797@126.com (Xuekun Tang), luoxianping9491@163.com (X. Luo)

Abstract: The similarity in floatability between molybdenite (MoS_2) and galena (PbS) poses a significant challenge for the efficient separation of these minerals in mineral processing. Regarding this issue, the current research systematically evaluates the selective inhibition effect and interfacial regulation mechanism of maleic acid–acrylic acid copolymer (MLA), a green and environmentally friendly inhibitor, in a kerosene-based flotation system. Through a series of comprehensive experimental investigations—including single-mineral and artificial mixed-mineral micro-flotation tests, contact angle measurements, Fourier transform infrared spectroscopy (FTIR) analysis, and X-ray photoelectron spectroscopy (XPS) analysis—the differential adsorption behavior of MLA on these two minerals has been clearly elucidated. The experimental results show that under specific conditions—namely a pH of approximately 8, an MLA concentration of 8 mg/L, and a kerosene concentration of 30 mg/L—there is a significant difference in the flotation behavior of the two minerals. The recovery of galena decreases sharply from 89.13% to below 2%, whereas the recovery of molybdenite remains consistently above 95%. This result effectively achieves a high degree of separation selectivity between the two minerals. Contact angle measurements further indicate that MLA significantly enhances the hydrophilicity of the galena surface, while exerting negligible influence on molybdenite. In conclusion, this study clearly demonstrates that MLA acts as an effective inhibitor for galena and enables efficient recovery of molybdenite through selective coordination and precise regulation of interfacial wettability. These findings provide not only a solid theoretical foundation but also valuable practical guidance for the green flotation separation of complex sulfide mineral systems and the development of novel low-toxicity inhibitors. This research therefore makes a significant contribution to advancing mineral processing technology and promoting environmental sustainability in the mining industry.

Keywords: molybdenite, galena, flotation, depressant, mineral separation, MLA

1. Introduction

Molybdenum, renowned for its exceptional high-temperature strength and outstanding corrosion resistance, is extensively employed across critical sectors such as aerospace, defense systems, energy production, chemical processing, and electronics, underscoring its status as a strategically vital metal for the advancement of modern industry (Yi et al., 2021; Qi et al., 2026). Molybdenite remains the predominant primary ore mineral for molybdenum extraction and metallurgical processing (Qi et al., 2026). Molybdenite is predominantly hosted in porphyry copper-molybdenum deposits (e.g., the Bingham Canyon and Chuquicamata deposits, USA and Chile, respectively) and polymetallic sulfide

DOI: 10.37190/ppmp/242673

deposits (e.g., the Jinduicheng molybdenum deposit, China), where galena commonly occurs as a co-genetic sulfide mineral (John., 1978; Borden., 2003; Zentilli et al., 2018). Molybdenite exhibits inherently high natural hydrophobicity, rendering froth flotation the dominant and economically optimal industrial process for its concentration (Yi et al., 2021). In practical industrial practice, non-polar collectors (e.g. kerosene, diesel) are routinely used as collectors for molybdenite, which can absorb on the basal planes of molybdenite, thereby increasing surface hydrophobicity (Yi et al., 2021; Qi et al., 2026). Galena, a ubiquitous sulfide mineral, frequently co-occurs with molybdenite in these ore deposits (Yang et al., 2025). Galena also exhibits intrinsic floatability due to its naturally hydrophobic surface (Yang et al., 2025; Zheng et al.,2021). Inevitably, in the absence of effective depressants, galena co-floats with molybdenite during flotation process leading to both grade dilution in the molybdenum concentrate and an unacceptable elevation in lead content (Zeng et al., 2024; Zhai et al., 2024; Tang et al., 2025). In the smelting process of molybdenum, the presence of lead impurities may bring multiple negative impacts. It not only reduces the performance indicators of the final alloy material, but also exacerbates the risk of atmospheric pollution due to the volatility of lead oxides at high temperatures (Tang et al., 2025). Obviously, the addition of depressants with high selectivity is essential in flotation process to enhance the separation of molybdenite and galena (Zhai et al., 2024; Tang et al., 2025).

Historically, inorganic depressants such as sulfur dioxide and dichromate (Fornasiero and Ralston,2005) have been widely employed in the industry for the separation of the PbS–MoS_2 system. These reagents operate by modifying the pulp's redox potential or forming insoluble, hydrophilic films on galena surfaces. However, these chemicals are highly toxic, corrosive, and environmentally hazardous, often causing equipment corrosion and subsequent challenges in water treatment, thereby limiting their applicability in green mineral processing and sustainable development. In recent years, organic and polymeric depressants have garnered increasing attention due to their environmental compatibility and biodegradability. Carboxyl-containing organic compounds, including citric acid (Apelblat, 2014), tartaric acid (Jantwal et al., 2022), carboxymethyl cellulose (CMC) (Benchabane and Bekkour, 2008), and polyacrylic acid (PAA) (Maurer et al., 2018), have been shown to modulate the surface charge of minerals through coordination or electrostatic adsorption, thereby enabling selective depression of galena. Nevertheless, these reagents often suffer from a limited number of functional sites, high sensitivity to pulp conditions, and inconsistent depressing performance.

In this context, copolymer depressants bearing multiple carboxyl groups (Ren et al., 2022) have demonstrated considerable potential for interfacial regulation due to their excellent water solubility, tunable molecular structure, and capacity for multi-site interactions. Compared with individual monomeric reagents, maleic acid–acrylic acid copolymer (MLA) incorporates carboxyl-containing units derived from both maleic acid and acrylic acid into a single polymer chain, providing multiple potential adsorption sites and opportunities for multidentate interactions with metal ions on mineral surfaces. Its polymeric structure may also facilitate the formation of a hydrated interfacial layer, thereby enhancing the hydrophilicity of the targeted mineral surface. These structural characteristics suggest that MLA could provide more stable surface adsorption and effective depression than its individual monomeric components under suitable flotation conditions. MLA (Qiu and Mao, 2013), which contains abundant carboxyl functional groups, may interact with metal sites on mineral surfaces through coordination and other interfacial interactions, thereby modifying surface wettability and flotation behavior. However, systematic investigations into the adsorption behavior and selective depression mechanism of MLA in the molybdenite–galena flotation system remain limited.

Based on this, the present study focuses on MLA as the research subject. By employing micro-flotation tests, contact angle measurements, FTIR(Riaz et al., 2018), XPS(Andrade, 1985), and other characterization techniques, we systematically investigate its selective depression behavior and mechanism toward molybdenite and galena from both macroscopic flotation performance and microscopic interfacial reaction perspectives. This study aims to elucidate the specific adsorption mechanism of MLA on galena surfaces, reveal the fundamental basis of its selective depression, and provide theoretical support and technical pathways for the molecular design of green and efficient flotation reagents (Nagaraj and Farinato, 2016), as well as for the development of clean mineral processing technologies for sulfide ores.

2. Experimental materials and methods

2.1. Preparation of mineral samples and sources of reagents

The high-purity molybdenite and galena samples used in the experiments were obtained from mineral deposits in Jiangxi and Hubei provinces, respectively. The mineral lumps, each with a purity exceeding 90%, were initially obtained through hand-sorting. The samples were subsequently crushed using a jaw crusher and then finely ground through dry processing in a ceramic ball mill. The resulting powders were subjected to dry sieving to obtain particles within the size fraction of −74+38 μm for micro-flotation tests. In these tests, kerosene was used as the collector, MIBC as the frother, and MLA as the depressant. All experiments were performed using deionized water. The maleic acid–acrylic acid copolymer (MLA) depressant was purchased from Qingdao Fumaisi Chemical Co., Ltd. (maleic acid–acrylic acid copolymer, solid content 48%, batch No. 139614001083) and used as received. No further purification was performed.

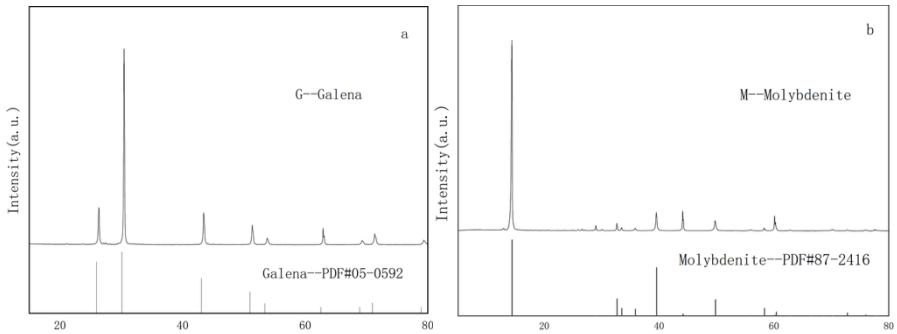


Fig. 1. XRD patterns of galena (a) and molybdenite (b) pure minerals.

2.2. Micro-flotation tests

A mixture of 1.0 g of molybdenite and 1.0 g of galena was used as the feed material for micro-flotation tests, which were conducted using a flotation machine (Model XFGII5, Jilin Exploration Machinery Plant) equipped with a 40 mL plexiglass cell. The impeller speed was maintained at 1800 rpm for all tests. Prior to flotation, 2.0 g of the mineral sample was placed in a 100 mL beaker containing 30 mL of distilled water and pre-cleaned using an ultrasonic bath for 5 minutes. After the supernatant was removed, the treated sample was transferred to the flotation cell with a total volume of 30 mL of water. The pulp pH was then adjusted to the desired value using dilute HCl or NaOH solutions. An appropriate dosage of depressant was then added to the pulp and conditioned for 5 minutes, after which specified amounts of kerosene and MIBC were added, followed by an additional 3 minutes of conditioning. Following this pretreatment, flotation was conducted for 3 minutes. Subsequently, the concentrate and tailings were collected, dried, and weighed. The recovery of individual pure minerals was calculated based on the mass percentage of the floated product. For the artificially mixed minerals, recovery was determined by assaying the Mo and Pb contents in both the concentrate and tailings. All flotation tests were conducted in triplicate to obtain representative average recovery values.

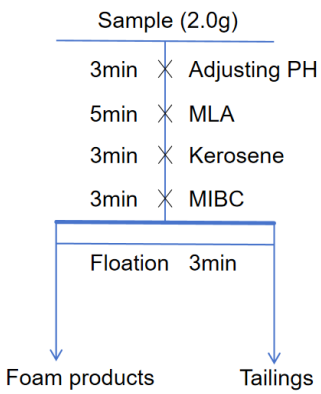


Fig. 2. Schematic diagram of the flotation test process for single minerals and mixed ores

2.3. Measurement contact angles on mineral surfaces

High-purity massive molybdenite and galena samples were mounted using analytically pure epoxy resin adhesive to ensure structural stability during subsequent preparation and analysis. Owing to the strong anisotropy of molybdenite, its basal (0001) plane is naturally hydrophobic while edge planes are hydrophilic. During the subsequent grinding and polishing steps, molybdenite preferentially cleaves along the basal plane due to its layered crystal structure; therefore, the final polished surface is dominated by the basal plane, with only a negligible contribution from edge planes. After curing, the samples were sequentially ground using 400-, 800-, and 1200-grit silicon carbide papers (or metallographic papers of equivalent specification) to remove surface impurities and the defective layer, thereby achieving the flatness required for fine polishing. Following coarse grinding, the samples were finely polished using a Tegramin-25 automatic polishing system: first with a 3 μm diamond suspension to reduce surface roughness, and then with a 1 μm diamond suspension until a mirror-like finish free of visible scratches was achieved. After polishing, the samples were rinsed five times with deionized water (resistivity ≥18.2 MΩ·cm) to remove residual polishing compounds and abrasive particles. They were then subjected to the standard pretreatment procedure employed in the flotation tests of this study (including pH adjustment and reagent conditioning) to ensure that surface conditions were consistent with those of the actual flotation environment. Finally, the samples were dried in a low-temperature environment (40–60 °C) under a stream of high-purity nitrogen (≥99.999%) to prevent surface oxidation and contamination. Consequently, the contact angles measured for molybdenite in this study primarily reflect the wettability of the basal plane, avoiding ambiguity caused by edge plane exposure. For galena (an isotropic mineral), the same polishing procedure yields a representative surface without the need for orientation selection. All tests were conducted in triplicate, and the reported data represent the arithmetic mean of three independent measurements to ensure reliability and reproducibility.

2.4. FTIR measurements

Fourier-transform infrared (FTIR) spectra of the mineral samples were acquired using a Spectrum Two spectrometer (PerkinElmer, USA) at a resolution of 4 cm^{-1}. Transmission spectra were obtained using the KBr pellet method, with background correction performed using a pure KBr pellet. For sample preparation, mineral powder was homogeneously mixed with spectroscopic-grade KBr at a mass ratio of 1:100 (1 mg sample to 100 mg KBr). All spectra were recorded in the wavenumber range of 4000–400 cm^{-1} under ambient conditions (25 ± 1 °C).

2.5. XPS measurements

XPS analysis was performed on an ESCALAB 250XI photoelectron spectrometer (Thermo Fisher Scientific, USA) using monochromatic Al Kα radiation (hν = 1486.6 eV) as the excitation source. All samples—including DTC-PAA, DTC-PAA/Pb^{2+} complexes, and MLA-treated and untreated galena specimens, which were also used in the FT-IR experiments described in Section 2.4—were analyzed under an analytical chamber vacuum of better than 1×10^{-9} Torr. Survey scans were acquired over a binding energy range of 0–1200 eV with at least three accumulations, an energy step size of 1.0 eV, and a pass energy of 100.0 eV. The C 1s peak at a binding energy (B.E.) of 284.6 eV was used for energy scale calibration. High-resolution spectra of the N 1s, S 2p, and Pb 4f regions were processed and fitted using XPS Peak 4.1 software.

3. Results and discussion

3.1. Micro-flotation results

3.1.1. The single mineral flotation behaviors of molybdenite and galena

To systematically evaluate the regulatory effect of MLA on the flotation behavior of galena (PbS) and molybdenite (MoS_2), micro-flotation tests were conducted at a fixed kerosene concentration of 30 mg/L and an MIBC concentration of 10 mg/L.

Fig. 3(a) illustrates the influence of pH on the recovery of both minerals. Across the tested pH

range, molybdenite recovery remained stable, whereas galena recovery consistently remained low. The maximum recovery difference between the two minerals was observed at pH ≈ 8, indicating optimal conditions for their selective separation.

Fig. 3(b) shows the effect of MLA concentration on mineral recovery. When the MLA concentration was increased to 8 mg/L, galena flotation was significantly suppressed, accompanied by a sharp decline in recovery, whereas molybdenite recovery remained largely unaffected and stayed high. This concentration was identified as the critical condition for effective separation between galena and molybdenite. In summary, under the optimized conditions of 30 mg/L kerosene, 10 mg/L MIBC, 8 mg/L MLA, and pH = 8, highly efficient flotation separation of galena and molybdenite can be achieved.

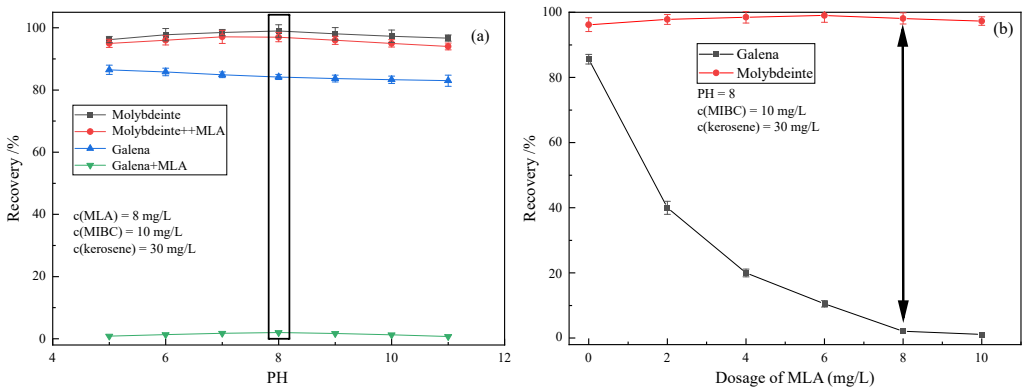


Fig. 3. The impact of MLA on the flotation recovery rates of molybdenite and galena under (a) varying pH conditions and (b) different MLA dosage levels

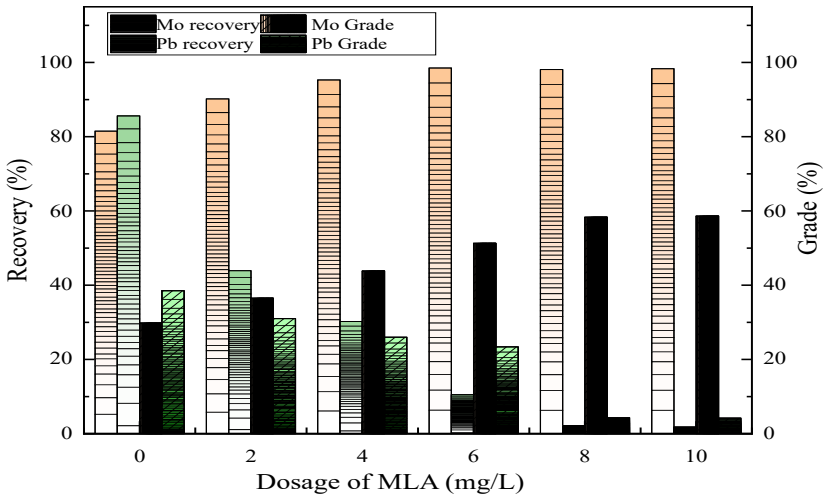


Fig. 4. The influence of MLA on the separation of molybdenite and galena binary mixed ore Flotation indexes

As shown in Fig. 4, the flotation separation results of the artificial molybdenite–galena mixture are presented as a function of MLA concentration. To evaluate the separation performance of MLA in a practical flotation system, binary mixed mineral flotation tests were conducted under fixed conditions of pH = 8, 30 mg/L kerosene, and 10 mg/L MIBC to maintain a stable flotation environment, while systematically investigating the selective separation mechanism and efficiency of MLA for the two minerals. As the MLA concentration increased from 0 to 8 mg/L, both the recovery and grade of galena in the concentrate significantly decreased, whereas those of molybdenite gradually increased. At an MLA dosage of 8 mg/L, the recovery of molybdenum in the concentrate exceeded 95%, whereas the lead recovery dropped to 3.25%. Further increasing the MLA dosage to 10 mg/L did not result in a significant improvement in either molybdenum recovery or grade. In summary, an MLA concentration of 8 mg/L was determined to be the optimal dosage for achieving efficient separation of molybdenite from galena in this system.

3.2. Contact angle analysis

To elucidate the selective depression mechanism of MLA, systematic contact angle measurements were performed on natural molybdenite and galena samples. In their natural state, the contact angles of molybdenite and galena were 83.1° and 70.3°, respectively. After treatment with kerosene, these values increased to 98.1° for molybdenite and 83.3° for galena, resulting in a difference of 14.8°, indicating that kerosene alone is insufficient as a collector for achieving effective flotation separation.

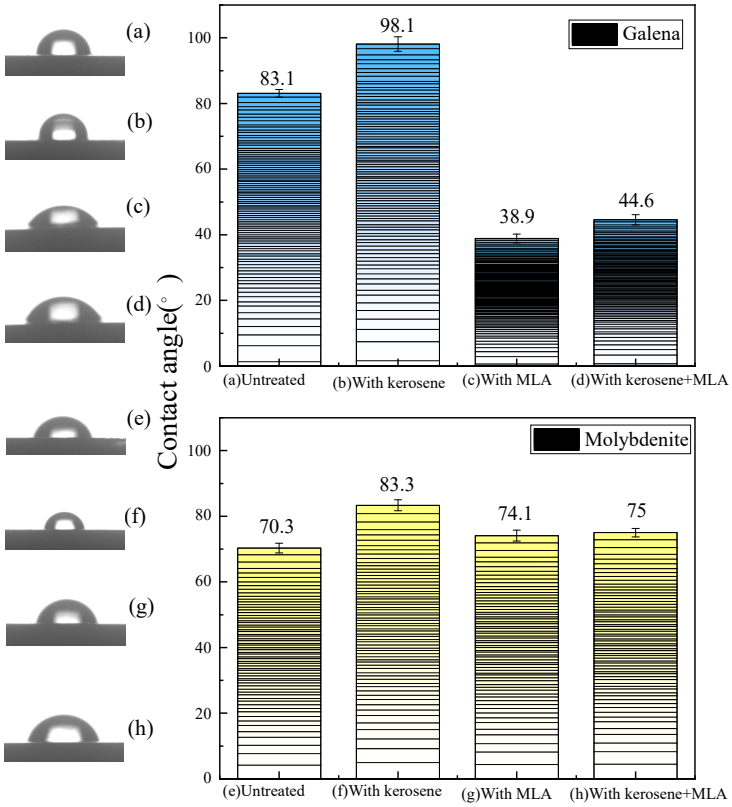


Fig. 5. The changes in contact angles of molybdenite and galena after the action of different reagents

However, contact angle measurements clearly revealed the selective wettability modification induced by MLA. As shown in Fig. 5, after MLA treatment, the galena surface transitioned from hydrophobic to hydrophilic (contact angle: 38.9°), whereas the hydrophobicity of molybdenite was largely preserved (contact angle: 74.1°). The considerable contact angle difference of 35.2° between the two minerals provides an ideal wettability window for effective flotation separation, demonstrating that MLA selectively enhances the hydrophilicity of the galena surface. Furthermore, when kerosene was introduced after MLA pretreatment, the contact angle of molybdenite recovered to 75°, close to the value obtained with kerosene alone. In contrast, the contact angle of galena only increased to 44.6°, indicating that the hydrophilicity induced by MLA treatment is not readily reversible upon kerosene addition. These results confirm the selective adsorption of MLA on the galena surface, which enhances its hydrophilicity while having minimal impact on the hydrophobicity of molybdenite. This creates a significant wettability contrast, providing strong evidence for the highly efficient flotation separation of molybdenite from galena. Preferential adsorption on edge sites. Molybdenite crystals inevitably possess a small fraction of edge planes (hydrophilic) even on a polished surface. MLA may preferentially adsorb onto these edge sites through coordination with undercoordinated Mo or S atoms, thereby slightly reducing the overall surface hydrophobicity. The basal plane, however, remains largely unaffected. Such edge-dominated adsorption would not be readily captured by FTIR or XPS when analyzing a basal-plane-dominated area. Therefore, the minor change observed on molybdenite does not contradict the conclusion that MLA selectively chemisorbs on galena but not on molybdenite. The key distinction lies in the magnitude of wettability modification ($\Delta\theta \approx 9°$ for molybdenite vs. $\Delta\theta \approx 44°$ for galena) and the presence of clear spectroscopic evidence only for galena.

3.3. FTIR results

Fig. 6 presents the FTIR spectra of molybdenite and galena before and after MLA treatment, together with the spectrum of pure MLA. In the MLA spectrum, a characteristic peak at 837 cm^{-1} is attributed to –CH groups, while the C–O stretching vibration of –COOH appears in the 1400–1450 cm^{-1} range. The absorption peaks at 1723 cm^{-1} and 1407 cm^{-1} correspond to the asymmetric and symmetric stretching vibrations of the carbonyl group (C=O) in carboxyl groups, respectively. Additionally, the peak at 3407 cm^{-1} is associated with –OH stretching, confirming the presence of –COOH functional groups.

In the spectrum of galena treated with MLA, the peaks at 1705 cm^{-1} (C=O), 1406 cm^{-1} (C–O), and 1123 cm^{-1} (C–O–C) (Karakus et al., 2020) were significantly enhanced compared to those in untreated galena. These changes, together with distinct peak shifts and the emergence of new characteristic features, provide direct evidence of the interaction between MLA and the galena surface, demonstrating MLA's ability to modify the local chemical environment of the mineral substrate. In contrast, no new characteristic peaks were observed for molybdenite after MLA treatment, indicating the absence of stable chemical adsorption of MLA on its surface.

In summary, FTIR analysis confirms that MLA chemically adsorbs onto the galena surface through $-COO^-$ groups, whereas no such chemical interaction occurs with molybdenite.

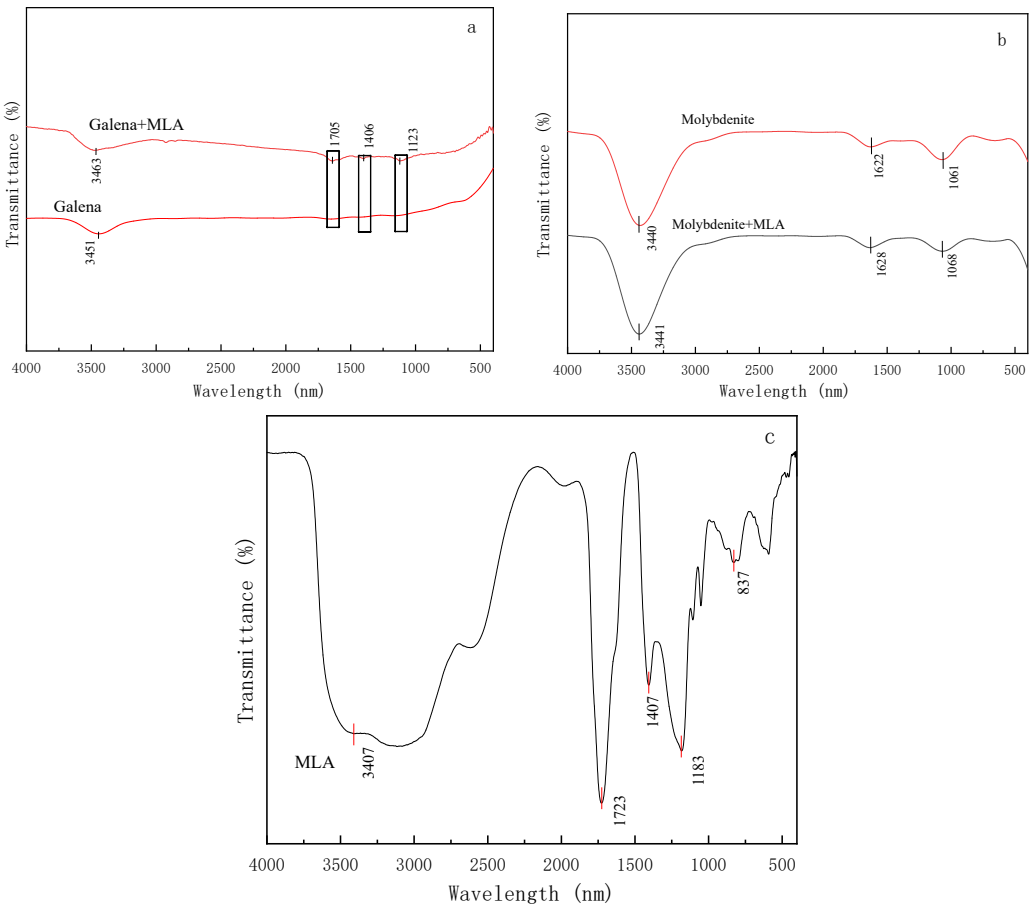


Fig. 6. The FTIR spectra of galena(a) and molybdenite(b) before and after MLA treatment and the FTIR spectra of MLA(c)

3.4. XPS results

Fig. 7(b) displays the high-resolution O 1s XPS spectra of galena before and after MLA treatment. The fitting results indicate that the O 1s peak can be deconvoluted into two components: a Metal–O peak at 531.4–531.5 eV and an O–C=O peak at 533.3–533.6 eV [19]. After MLA treatment, a new peak appeared at 529.74 eV, which is attributed to the O–C=O group within the molecular structure of MLA.

XPS analysis provides direct evidence for the chemical adsorption of MLA on the galena surface. The appearance of a new O–C=O peak in the O 1s spectrum, together with the systematic shift in binding energy of the Pb 4f orbitals, collectively indicates that the deprotonated carboxyl groups (–COO^-) (Zhang and Liu, 2000) formed stable inner-sphere complexes with surface Pb^{2+} ions. This interaction altered the chemical environment of surface oxygen species, leading to a significant increase in peak intensity in the high-binding-energy region.

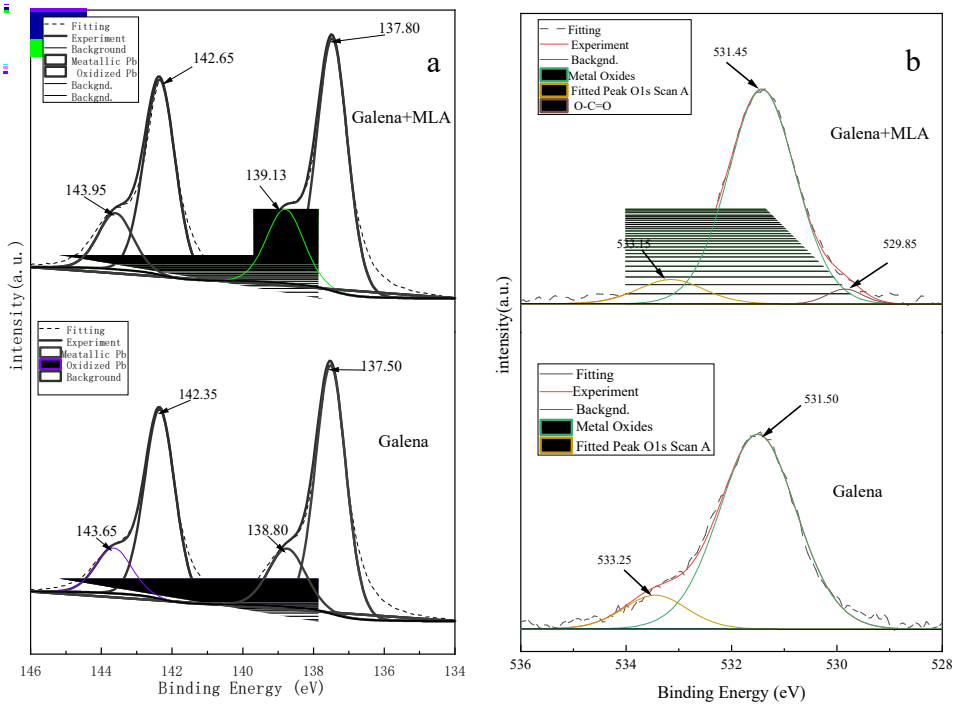


Fig. 7. XPS spectra of galena before and after MLA treatment: (a) O 1s spectra and (b) Pb 4f spectra

Fig. 7(a) shows the high-resolution Pb 4f XPS spectra of galena before and after MLA treatment. In the Pb 4f spectrum, the characteristic peaks at 137.50 eV and 138.80 eV are assigned to the Pb–S and Pb–O chemical states, respectively. After MLA treatment, these binding energies shifted slightly to 137.80 eV and 139.13 eV. This observation suggests that the adsorption of MLA on the galena surface is associated with coordination interactions between the carboxylate groups (–COO^-) of MLA and surface Pb sites, thereby modifying the surface chemical environment and enhancing its hydrophilicity. The results further confirm that MLA molecules undergo chemical adsorption on the galena surface. After MLA treatment, the Pb 4f spectrum exhibited two notable changes: first, the intensity of all spin–orbit split peaks decreased significantly, indicating a shielding effect of the MLA adsorption layer on the substrate Pb signal; second, the overall Pb 4f binding energy shifted to higher values (e.g., Pb $4f_{7/2}$ shifted to 137.80 eV and Pb $4f_{5/2}$ to 139.13 eV), which is attributed to reduced electron cloud density following the formation of chelate structures between MLA carboxyl groups and Pb^{2+}, resulting in diminished photoelectron shielding.

Comprehensive analysis reveals that during the adsorption of MLA on the galena surface, it displaces pre-adsorbed hydroxyl groups or water molecules, forming a negatively charged organic layer that transforms the surface from hydrophobic to hydrophilic. Simultaneously, this layer inhibits further adsorption of collectors through electrostatic repulsion and steric hindrance, thereby significantly reducing the floatability of galena. In contrast, the limited coordination capability of metal sites on the molybdenite surface leads to minimal adsorption of MLA, resulting in negligible impact on its floatability.

In summary, the appearance and enhancement of the O–C=O peak in the O 1s spectrum directly confirm that MLA adsorbs onto the galena surface in the form of carboxylate groups. The mechanism follows a "carboxyl deprotonation–metal coordination–surface hydrophilization" pathway, achieving chemical depression of galena. This mechanism is consistent with the selective depression behavior

observed in flotation experiments, indicating that the suppression of galena by MLA fundamentally arises from interfacial chemical complexation and surface property modulation.

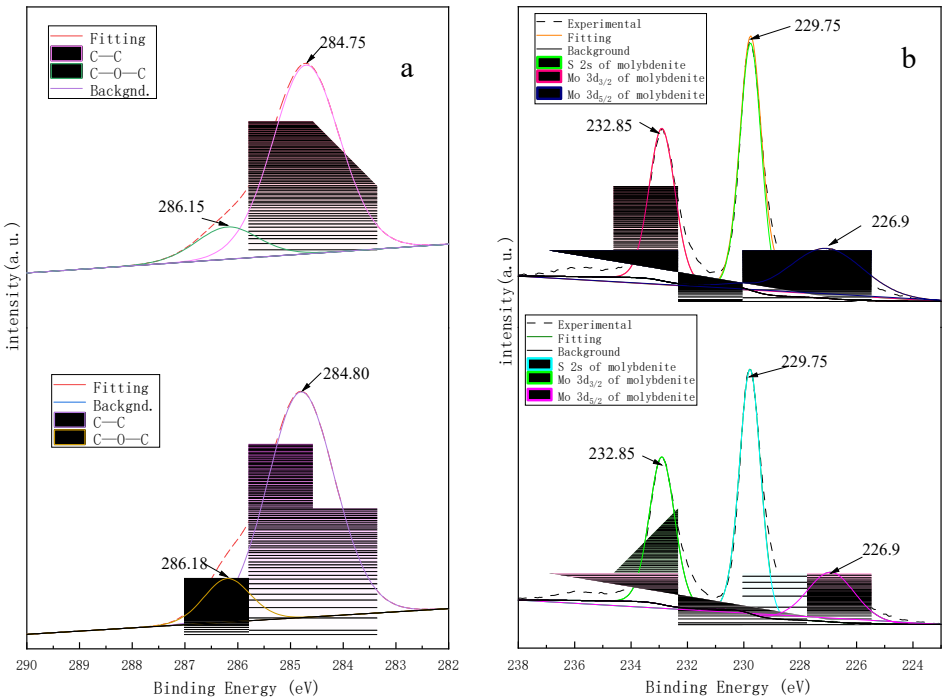


Fig. 8. XPS spectra of molybdenite before and after MLA treatment: (a) O 1s spectra and (b) Mo 3d spectra

To further investigate the effect of MLA treatment on the surface elemental composition of molybdenite and galena, XPS analysis was performed to compare the surface characteristics of treated and untreated samples. For the pure molybdenite sample, the O 1s spectrum (Fig. 8a) of the untreated molybdenite exhibited characteristic peaks corresponding to hydroxide, MoO_3 (Zang et al.,2025), and organic oxygen species at binding energies of approximately 531.55 eV, 532.45 eV, and 530.55 eV, respectively. After MLA treatment, the positions and shapes of these oxygen-related peaks showed negligible changes, indicating that MLA has minimal influence on the oxygen-containing chemical states on the molybdenite surface.

In the Mo 3d and S 2s spectra (Fig. 8b), untreated molybdenite displayed distinct characteristic peaks for Mo 3d, S 2s, and other related species at specific binding energies. Following MLA treatment, the spectral profiles of Mo 3d and S 2s, including both peak positions (e.g., the prominent peaks of untreated molybdenite near 232.85 eV and 229.75 eV, and those of MLA-treated molybdenite near 232.90 eV and 229.95 eV) and relative intensities, remained essentially unchanged.

Collectively, these XPS results demonstrate the absence of significant chemical interactions between MLA and molybdenite, as the chemical states of key surface elements (Mo, S, O) were not markedly altered following MLA treatment.

3.5. The potential depression mechanism of MLA on galena

Based on flotation tests and surface analysis, this study elucidates the mechanism of the environmentally friendly depressant MLA in the flotation separation of molybdenite and galena. Under alkaline flotation conditions, MLA molecules dissociate to generate abundant carboxylate anions ($-COO^-$) that can chelate with divalent metal cations such as Pb^{2+}, providing the structural basis for selective adsorption on mineral surfaces. The galena surface, rich in active Pb^{2+} sites, enables chemical adsorption of MLA through the formation of stable Pb–O–C coordination structures via its carboxylate anions(Zhang et al.,2009). This process was confirmed by the appearance of new characteristic absorption peaks in the FTIR spectra and changes in the chemical environment of Pb observed in XPS analysis. The selective adsorption of MLA significantly enhances the hydrophilicity

of the galena surface, as evidenced by a marked decrease in contact angle. Even after the subsequent addition of the collector kerosene, the surface hydrophobicity could not be effectively restored, resulting in effective depression of galena flotation.

In contrast, the cleavage planes of molybdenite are primarily composed of chemically saturated sulfur atoms and lack available metal sites for coordination with MLA. Consequently, only weak physical adsorption occurs on the molybdenite surface, which is insufficient to alter its wettability or flotation behavior. Therefore, molybdenite maintains effective collector adsorption and good floatability following kerosene addition.

In summary, the distinct adsorption behaviors of MLA on galena versus molybdenite enable highly efficient and selective flotation separation of the two minerals, offering a promising technical approach for the green separation of polymetallic sulfide ores.

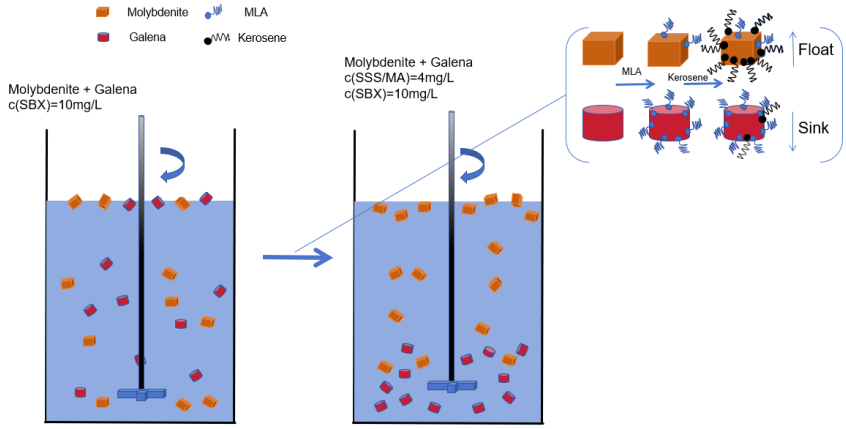


Fig. 9. The possible selective depression mechanism of MLA on molybdenite and galena

4. Conclusions

This study investigated the mechanism of the environmentally friendly depressant maleic acid-acrylic acid copolymer (MLA) in the flotation separation of molybdenite and galena. The results demonstrate that MLA exhibits significant selective depression toward galena, while having minimal impact on the floatability of molybdenite, indicating excellent depression capability and mineral selectivity. Under the optimized conditions of 8 mg/L MLA, 30 mg/L kerosene, and pH ≈ 8, highly efficient separation of molybdenite from galena was achieved. Contact angle measurements revealed that MLA adsorbs markedly on the galena surface, enhancing its hydrophilicity and reducing the subsequent adsorption of the collector. In contrast, MLA shows negligible adsorption on the molybdenite surface, where both wettability and hydrophobic behavior remain largely unaffected. FTIR analysis confirmed chemical bonding and hydrogen bonding interactions between MLA and the galena surface, whereas no distinct evidence of chemical adsorption was observed on molybdenite. XPS results further revealed that carboxyl groups in MLA form Pb–O–C coordination structures with Pb^{2+} sites on the galena surface, leading to changes in the surface electronic structure and preventing collector attachment. No analogous chemical interaction was detected on the molybdenite surface.

In summary, this work elucidates a novel selective depression approach utilizing a carboxyl-based copolymer. It is confirmed that MLA achieves nearly complete flotation separation in the MoS_2/PbS system by specifically coordinating with Pb^{2+} sites on the galena surface, thereby forming a hydrophilic interfacial layer that effectively blocks collector adsorption. The revealed mechanism provides molecular-level insights for designing a new generation of green sulfide ore depressants, offering important theoretical support and practical guidance for the efficient and environmentally friendly flotation separation of complex sulfide ores.

Acknowledgments

The authors would like to thank the Jiangxi University of Science and Technology PhD Start-up Fund (No. 205200100645).

Reference

ANDRADE J.D., 1985, *X-ray photoelectron spectroscopy (XPS). Surface and interfacial aspects of biomedical polymers: volume 1 surface chemistry and physics*, 105–195.

APELBLAT A., 2014, *Citric acid*. Springer.

BENCHABANE A., BEKKOUR K., 2008, *Rheological properties of carboxymethyl cellulose (CMC) solutions*. Colloid and Polymer Science, 286(10), 1173–1180.

BORDEN R.K., 2003, *Environmental geochemistry of the Bingham Canyon porphyry copper deposit, Utah*. Environmental Geology, 43(7), 752–758.

CAO M., WANG L., LI A., YANG X., GONG X., XU J.T., LIU J., 2024, *Kinetics and scale inhibition application studies towards bulk and RAFT copolymerization of maleic anhydride and acrylic acid*. European Polymer Journal, 220, 113504.

FORNASIERO D., RALSTON J., 2005, *Cu (II) and Ni (II) activation in the flotation of quartz, lizardite and chlorite*. International Journal of Mineral Processing, 76(1–2), 75–81.

JANTWAL A., DURGAPAL S., UPADHYAY J., JOSHI T., KUMAR A., 2022, *Tartaric acid*. In Antioxidants effects in health (pp. 485–492). Elsevier.

JOHN E.C., 1978, *Mineral zones in the Utah Copper orebody*. Economic Geology, 73(7), 1250–1259.

KARAKUS G., CAN H.K., YAGLIOGLU A.S., 2020, *Synthesis, structural characterization, thermal behavior and cytotoxic/antiproliferative activity assessments of poly (maleic anhydride-alt-acrylic acid)/hydroxyurea polymer/drug conjugate*. Journal of Molecular Structure, 1210, 127989.

LIU Q., ZHANG Y., 2000, *Effect of calcium ions and citric acid on the flotation separation of chalcopyrite from galena using dextrin*. Minerals Engineering, 13(13), 1405–1416.

MAURER J.J., EUSTACE D.J., RATCLIFFE C.T., 1987, *Thermal characterization of poly (acrylic acid)*. Macromolecules, 20(1), 196–202.

NAGARAJ D.R., FARINATO R.S., 2016, *Evolution of flotation chemistry and chemicals: A century of innovations and the lingering challenges*. Minerals Engineering, 96, 2–14.

QI M., WANG P., PENG W., WANG W., CAO Y., ZHANG L., HUANG Y., 2026, *Selective flotation of chalcopyrite and molybdenite: A review of depressant applications*. Green and Smart Mining Engineering.

QIU Y.R., MAO L.J., 2013, *Removal of heavy metal ions from aqueous solution by ultrafiltration assisted with copolymer of maleic acid and acrylic acid*. Desalination, 329, 78–85.

REN F., LU Y., SUN B., WANG C., YAN J., LIN H., …, HAN S., 2022, *Structure regulation and influence of comb copolymers as pour point depressants on low temperature fluidity of diesel fuel*. Energy, 254, 124438.

RIAZ T., ZEESHAN R., ZARIF F., ILYAS K., MUHAMMAD N., SAFI S.Z., …, REHMAN I.U., 2018, *FTIR analysis of natural and synthetic collagen*. Applied Spectroscopy Reviews, 53(9), 703–746.

TANG H., ZHANG X., ZENG Y., HUA Z., SUN W., WANG L., JIANG F., 2025, *Robust adsorption of ellagic acid on galena surface for efficient flotation separation of molybdenite and galena.* Applied Surface Science, 686, 162117.

YANG S., LUO X., TANG X., LIU Z., CHEN R., FAN X., …, SHEN L., 2025, *Selective adsorption of hydrolized polymaleic anhydride as an eco-friendly depressant on galena during the flotation of molybdenite: Experimental and DFT study*. Colloids and Surfaces A: Physicochemical and Engineering Aspects, 137853.

YI G., MACHA E., VAN DYKE J., MACHA R.E., MCKAY T., FREE M.L., 2021, *Recent progress on research of molybdenite flotation: A review*. Advances in Colloid and Interface Science, 295, 102466.

ZANG B., CHEN B., GAO X., YAO D., CHEN J., LU C., 2025, *Synergistic flame retardant mechanism of MoO_3 and intumescent flame retardants: Insights from real-time char layer resistance monitoring*. Thermochimica Acta, 749, 180013.

ZENG Y., DONG Y., ZHANG X., HUA Z., WU X., SUN W., …, TANG H., 2024, *Enhancement of Mo-Pb flotation separation using gallic acid as a molybdenite depressant: Investigating flotation behavior and mechanism*. Journal of Molecular Liquids, 416, 126460.

ZENTILLI M., MAKSAEV V., BORIC R., WILSON J., 2018, *Spatial coincidence and similar geochemistry of Late Triassic and Eocene–Oligocene magmatism in the Andes of northern Chile: evidence from the MMH porphyry type Cu–Mo deposit, Chuquicamata District*. International Journal of Earth Sciences, 107(3), 1097–1126.

ZHAI Q., DONG W., LIU R., XIE Z., CAO Z., SUN W., 2024, *Green separation of galena from molybdenite by flotation using DL-dithiothreitol as a depressant*. Separation and Purification Technology, 347, 127676.

ZHANG L., LI Z.J., LIN Q.P., QIN Y.Y., ZHANG J., YIN P.X., …, YAO Y.G., 2009, *Synthesis, structure, and luminescent properties of hybrid inorganic−organic framework materials formed by lead aromatic carboxylates: inorganic connectivity variation from 0D to 3D*. Inorganic Chemistry, 48(14), 6517–6525.

ZHENG M., PENG T., WANG Y., LUO L., SHAO W., GAO J., LU Q., 2021, *Flotability of galena and pyrite using 2-mercaptobenzimidazole as a chelating agent: Adsorption characteristics and flotation mechanisms*. Powder Technology, 393, 449–460.